Synthesis of MoS$_2$@TiO$_2$ Nanosheets by Liquid Exfoliation Method for Wastewater Treatment

Shweta[a], Pooja Singh[a], Vinamrita Singh[b], Kaushal Kumar[a], Sohan Lal[c], & Arun Kumar[a*]

[a]Department of Physics, J C Bose University of Science and Technology, YMCA, Faridabad 121 006, India
[b]Department of Physics, Netaji Subhas University of Technology, East Campus, Delhi 110 031, India
[c]Department of Physics, National Institute of Technology, Kurukshetra 136 119, India

Molybdenum Disulphide (MoS$_2$) based materials in pure form or composites are known for their photocatalytic activity including wastewater treatment and purification. In the present study, pristine MoS$_2$ nanosheets and MoS$_2$@TiO$_2$ composite nanosheets are synthesized via grinding-assisted sonication process with N-Methylpyrrolidone (NMP) as solvent. TiO$_2$ being environment friendly with high photochemical stability, provides a suitable reinforcement material for photocatalytic applications. The prepared dispersions are characterized by UV-Vis, Raman and FTIR spectroscopy for structural and optical properties. These nanosheets are tested for methylene blue dye degradation in dark and in the presence of sunlight at intervals of 30 minutes. The MoS$_2$@TiO$_2$ nanosheets show enhanced degradation efficiency in comparison to the pristine MoS$_2$ nanosheets. These composite nanosheets are potential materials in tackling dye pollutants for application in wastewater treatment plants and purification.

Keywords: Photocatalytic activity, Methylene blue, Water treatment, Nanosheets, Composite

1 Introduction

A global, non-negligible environmental issue is the water pollution due to industrial effluents containing synthetic chemical dyes which are toxic for human health.[1] The dyes pose a threat to healthy living and therefore, degradation of the harmful components in wastewater is a serious concern of current research. In this context, solar driven semiconductor photocatalysts have gained interest of researchers as the irradiation of 1.5×10^{18} kW h solar energy reaching earth every year is nearly 28,000 times the global energy consumption per year.[2] The two-dimensional transition metal dichalcogenides (TMDs) are emerging materials with enhanced photocatalytic, photovoltaic, and optoelectronic properties. 2D nanomaterials have more beneficial properties like high anisotropy and good chemical stability due to quantum confinement of electrons as compared to bulk materials. Among these, Molybdenum Disulphide (MoS$_2$), has attracted attention as a potential photocatalyst. The captivating properties of MoS$_2$ include earth abundance, chemical stability, good catalytic property, active edge sites, high specific area, large exciton binding energy, transition of energy band gap from indirect (~1.2 eV)

in bulk form to direct (~2.3 eV) in 2D form and hence strong absorbance in visible spectrum.[3,4]

In layered crystal MoS$_2$ structure, there is a strong covalent bonding between transition metal Mo and chalcogen atoms S, and each MoS$_2$ layer is bonded weakly by van der Waals forces to nearby layers that is responsible for the above-mentioned properties of MoS$_2$.[5-7]

Degradation of chemical dyes is at utmost priority to save the ecosystem from getting contaminated. 2D MoS$_2$ is a promising photocatalytic material with good visible light response. Since solar driven photocatalysis includes a wide spectrum of radiations, incorporating another good photocatalyst with MoS$_2$, say titanium dioxide (TiO$_2$), would expand the utilization of solar spectrum and hence more efficient elimination of pollutants from wastewater. In 1972, Fujishima & Honda first used TiO$_2$ as a photocatalyst and thereafter, many researchers worked on this material. TiO$_2$ has a band gap of 3.2 eV and thus good absorbance in UV range while 2D MoS$_2$ has good visible light response due to a band gap of ~ 1.9 eV- 2.3 eV.[8] Zhou *et al.*[9] reported many MoS$_2$ based heterostructures for improved photocatalytic performance and concluded that MoS$_2$ and TiO$_2$ composites are promising alternative for better photocatalytic applications.

Corresponding author (E-mail: arunkumar@jcboseust.ac.in)

Notably, the photocatalytic dye degradation performance of MoS_2 alone and of TiO_2 on adding MoS_2 has been investigated till date but change in MoS_2 response on reinforcing TiO_2 has not been widely explored.[10-11] In this context, we have prepared pristine MoS_2 nanosheets and TiO_2 reinforced MoS_2 nanosheets for comparative study in the degradation of methylene blue dye. The nanosheets are successfully exfoliated via manual grinding followed by probe sonication method. The prepared nanosheets are characterized for optical, structural and photocatalytic properties. Interestingly, it is observed that TiO_2 reinforced MoS_2 showed improved dye degradation within 180 minutes in comparison to pristine MoS_2. The outcomes of this study anticipate that the nanosheets of MoS_2 along with its composites or heterostructures are promising materials for photocatalytic degradation of harmful dye effluents into non-harmful compounds like CO_2 and O_2.

2 Materials and Methods

2.1 Materials

MoS_2 bulk powder with APS 60-70 μm, purity 99.9% and TiO_2 Anatase with APS 10-25 nm, purity 99.9% were procured from Nanoshel. N-Methylpyrrolidone (NMP) solvent was purchased from CDH, with 99% purity. Methylene blue (MB) was purchased from Qualikems. Distilled water is used to prepare the dye solutions. All materials are analytical grade and were used as received.

2.2 Synthesis of MoS_2 nanosheets

MoS_2 bulk powder weighing 1g is crushed manually in an agate mortar pestle for 4 hours duration. NMP solvent is added dropwise (~0.5 ml) for grinding. The grounded powder is dried overnight in a hot air oven at 60 °C to evaporate the solvent. In 20 ml of NMP, the MoS_2 powder is poured and stirred at 1000 rpm for 2 hours followed by probe sonication (LABSONIC Probe Sonicator, 1200W) for 2 hours at 5 °C with 5s on and 2s off state to avoid heating. It is then kept undisturbed overnight for sedimentation and then centrifuged at 5000 rpm for 30 minutes. Top $2/3^{rd}$ portion of supernatant is decanted called the pristine MoS_2 dispersion consisting of nanosheets.

2.3 Synthesis of MoS_2@TiO_2 nanosheets

1g of MoS_2 bulk powder and 0.04g of TiO_2 anatase are grounded manually with 0.5 ml NMP each in separate mortar pestle for 4 hours. Further, both the powders are dried overnight in oven at 60°C. The two dried powders are then mixed together in 20 ml NMP solvent for 24 hours in a magnetic stirrer at 1000 rpm. It is then followed by probe sonication (LABSONIC Probe Sonicator, 1200W) for 2 hours with 8s on and 2s off in an ice-cold bath maintain temperature at 5°C. The sonicated solution is sedimented naturally overnight and then centrifuged at 5000 rpm for 30 minutes to separate out the lighter exfoliated nanosheets. The supernatant is decanted containing MoS_2@TiO_2 nanosheets.

2.4 Photocatalytic Experiment

Photocatalytic degradation of methylene blue dye (MB) is investigated under dark as well as in natural sunlight. A 20 ppm of MB dye solution is prepared by adding 5 mg MB in 250 ml distilled water. The dye solution is further divided equally in five 50 ml each solution. One of them is to be used without any photocatalyst for observing the self-degradation property of MB under natural sunlight. Under dark, 10 mg of MoS_2 and MoS_2@TiO_2 photo catalysteach are added in two dye solutions, one for experiment in dark and another for sunlight. All these four solutions are stirred in dark for 30 minutes at 500 rpm to attain adsorption/desorption equilibrium. The dye solutions are observed in dark and in sunlight separately for both the photocatalysts by collecting 3ml of solutions after every 30 minutes upto 180 minutes. The dye degradation response is estimated by recording the absorption spectra of the collected aliquots.

2.5 Characterizations

Structural analysis of MoS_2 and MoS_2@TiO_2 nanosheets is performed by FTIR spectroscopy (Perkin-Elmer Spectrum Two FT-IR spectrometer) in the range of 400 cm^{-1} to 4000 cm^{-1}. Raman spectra and Photoluminescence (PL) spectra of MoS_2 and MoS_2@TiO_2 nanosheets both are recorded by WITec – ALPHA300 RAS Microscope at 355 nm laser source. For Raman and PL, the suspensions are drop casted on clean glass slides and dried overnight in hot air oven at 60°C to remove the solvent. The absorption spectra of MoS_2, MoS_2@TiO_2nanosheets and collected dye aliquots is carried out by Shimadzu UV-3600i plus UV-VIS-NIR Spectrophotometer in the range of 300 nm to 800 nm.

3 Results and Discussion

3.1 FTIR spectroscopy

Structural analysis in terms of functional groups can be obtained from FTIR spectroscopy shown in

Fig.1. From Fig.1(a), it is seen that the characteristic peaks of bulk MoS_2 are all available in exfoliated MoS_2 too, with no emergence of new peaks. The peaks of MoS_2 nanosheets are bit broadened and blue shifted towards higher wave number in comparison to bulk MoS_2. The peaks corresponding to Mo-S vibration of 2D MoS_2 and bulk MoS_2 are positioned at 470 cm^{-1} and 460 cm^{-1}, respectively, although weak as shown in inset due to low concentration of MoS_2. The bond assigned to O-H bending vibrations is in the range from 1660 cm^{-1} to 1754 cm^{-1} in 2D MoS_2 and at 1648 cm^{-1} for bulk MoS_2. H-O-H stretching vibrations for exfoliated MoS_2 and bulk MoS_2 are located at 2955 cm^{-1} and 2930 cm^{-1} respectively. This can be attributed to residual stress while high energy exfoliation process leading to transition from 3D to 2D MoS_2.[4,12]This infers that no structural deformations occurred in 2D MoS_2 after high energy exfoliation process. Fig. 1(b) shows the FTIR spectrum of MoS_2@TiO_2 nanosheets. The transmittance bands from 400 cm^{-1} to 800 cm^{-1} (besides 467 cm^{-1} that corresponds to Mo-S stretching

Fig. 1 — FTIR spectra of (a) Bulk MoS_2 and MoS_2 nanosheets, (b) MoS_2@TiO_2 nanosheets.

vibration) are attributed to Ti-O and O-Ti-O bands. The bonds in the range 1400 cm^{-1} – 1675 cm^{-1} and another broad range from 3000 cm^{-1} to 3500 cm^{-1}can be assigned to O-H bending vibrations and H-O-H stretching vibrations respectively. This confirms the formation MoS_2 and TiO_2 heterostructure.[13,14]

3.2 Raman spectroscopy

Raman spectroscopy is helpful to estimate the efficiency of exfoliation in terms of number of layers in 2D MoS_2. In MoS_2, E_{2g}^1 and A_g^1 are the two vibration modes assigned to in-plane vibration and out-of-plane vibrations of Sulphur atoms, respectively. Figure 2(a) shows the locations of peaks E_{2g}^1 and A_g^1 for 2D MoS_2 at 384.48 cm^{-1} and 405.65 cm^{-1} with a frequency difference $\Delta k = 21.17$ cm^{-1} while E_{2g}^1 at 382.16 cm^{-1} and A_g^1 at 407.65 cm^{-1}with $\Delta k = 25.49$ cm^{-1} for bulk MoS_2.In literature, Δk is around 18 cm^{-1} -19 cm^{-1}for mono, 22 cm^{-1}for bi, 23 cm^{-1}-24 cm^{-1}for three, 25 cm^{-1}for four to five layers and 26 cm^{-1} for bulk MoS_2.[1,15]Thus, it confirms the well exfoliation of MoS_2 in mono or bi layer range along with sustained 2H type structure of MoS_2. Raman spectra of TiO_2 anatase, MoS_2 nanosheets and MoS_2@TiO_2 nanosheets is given in Fig. 2(b). The characteristic Raman modes of TiO_2 anatase are located at 142.1 cm^{-1} (E_g), 192.2 cm^{-1} (E_g), 394.5 cm^{-1} (B_{1g}), 516.6 cm^{-1} (A_{1g}+B_{1g}) and 638.6 cm^{-1} (E_g). The peaks E_g, B_{1g}, and A_{1g} are assigned to the symmetric stretching vibrations, symmetric bending, and antisymmetric bending vibrations of O–Ti–O bonds, respectively.[10,11] For MoS_2 nanosheets, the peak positions of Raman modes E_{2g}^1 and A_g^1 occur at 384.48 cm^{-1} and 405.65 cm^{-1} with a frequency difference of $\Delta k = 21.17$ cm^{-1}. The co-existence of small quantity of TiO_2 along with MoS_2 can be seen by existence of some of the TiO_2 peaks (although weak) 520.5 cm^{-1} (A_{1g}+B_{1g}) and 675.7 cm^{-1} (E_g) along with MoS_2peaks at 381.53 cm^{-1} (E_{2g}^1) and 405.65 cm^{-1} (A_g^1) with frequency difference 24.1 cm^{-1}. The B_{1g} peak is superimposed by the MoS_2 peaks and thus does not appear explicitly. Moreover, this superposition is responsible for increase in frequency spacing between peaks E_{2g}^1 and A_g^1 from 21.17 cm^{-1} to 24.1 cm^{-1}, still in 2D range.

3.3 PL analysis

PL spectra for bulk and sonicated MoS_2 in Fig. 2(c) clearly show the emergence of two emission peaks positioned at 460 nm and 540 nm for 2D MoS_2 while none for bulk MoS_2. This accounts for successful transition from indirect to direct energy band gap with
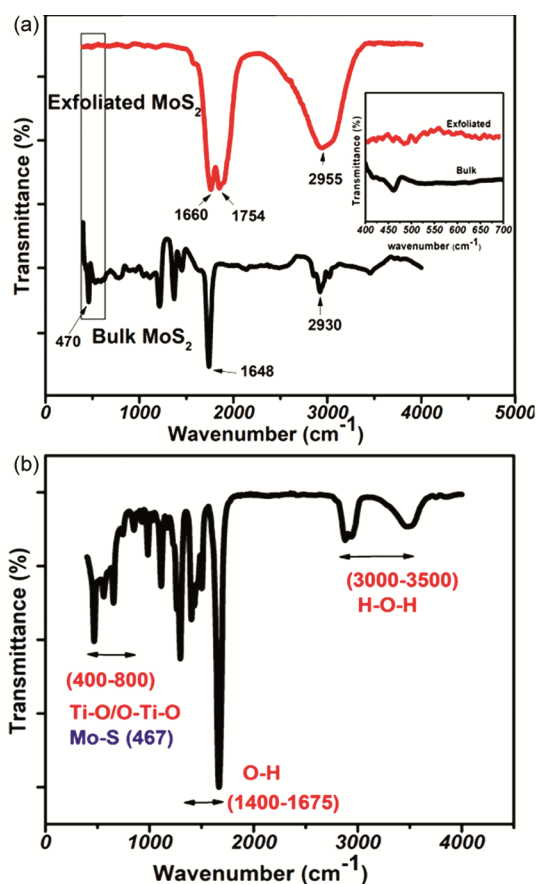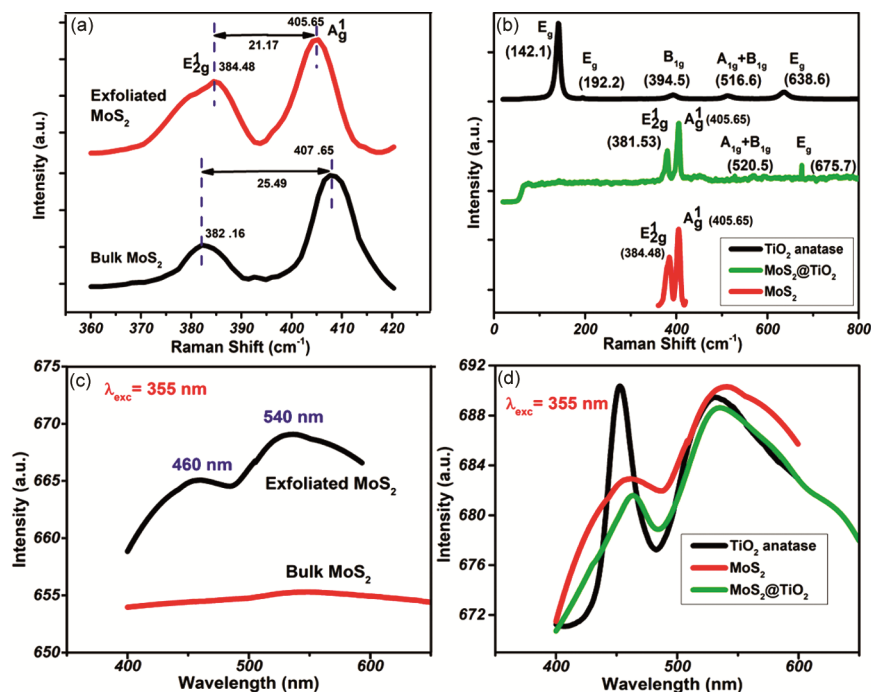
Fig. 2 — Raman spectra of (a) Bulk MoS_2 and MoS_2 nanosheets, (b) pure TiO_2 anatase, $MoS_2@TiO_2$ nanosheets and MoS_2 nanosheets. PL spectra of (c) Bulk MoS_2 and MoS_2 nanosheets, (d) pure TiO_2 anatase, $MoS_2@TiO_2$ nanosheets and MoS_2 nanosheets.

the two peaks assigned to A and B excitons for transitions at K-point in Brillouin zone.[16] Figure 2(d) shows the PL emission peaks of pure TiO_2 anatase, MoS_2 nanosheets and $MoS_2@TiO_2$ nanosheets around 452-460 nm and 530-540 nm. It indicates the direct band gap in 2D $MoS_2@TiO_2$ along with decrease in intensity implying depression in recombination of photo gene rated electron-hole pairs.[9,11] Thus, this composite can exhibit better photo catalytic performance.

3.4 UV-V is Spectroscopy

UV-Vis spectrum is an informative technique to look for the extent of absorption of photons which is an utmost requirement for a good photocatalyst. It is clearly shown in Fig. 3(a) the four absorption peaks in 2D MoS_2 peaks A- 668 nm, B- 608 nm corresponding to the smallest direct transition of the electrons from the top of valence band to bottom of conduction band, C- 447 nm and D- 398 nm arising from the direct transitions occurring from deep valence band to conduction band. While in bulk MoS_2, only A at 690 nm and B at 628 nm are observed. This accounts for enhanced absorption of visible light in 2D MoS_2. Moreover, there is a blue shift of 22 nm and 20 nm for peak A and B, respectively, in exfoliated MoS_2 compared to bulk MoS_2. In agreement to literature, this justifies for increase in energy band gap for few layer MoS_2.[17] From Fig. 3(b), it is seen that pure

TiO_2 has high absorbance in UV range, while pristine MoS_2 nanosheets absorb photons in visible range. In absorption spectrum of $MoS_2@TiO_2$, a small trace of red shift is observed. Thus, by incorporating TiO_2 in MoS_2, encompassing of UV range of solar spectrum along with visible light is possible, providing more active sites for photocatalytic reactions.[10]

Furthermore, energy band gap of both bulk and 2D MoS_2 is calculated using Tauc's relation $[(\alpha h\upsilon)^{\frac{1}{n}} = k(h\upsilon - E_g)]$, where $h\upsilon$ is incident optical energy, k proportionality constant, n has value ½ or 2 for direct or indirect band gap, respectively. α is known as absorption coefficient and can be calculated by relation $[\alpha = 2.303 \ log(A/d)]$, where 'A' shows optical absorbance and 'd' optical path length.[3] As shown in Fig.3(c), the E_g comes out to be 2.3 eV for exfoliated MoS_2 and 1.5 eV for bulk MoS_2 (shown in inset). Likewise, in Fig. 3(d), 2.4 eV for $MoS_2@TiO_2$ nanosheets (owing to small red shift in optical absorption spectrum) and 3.4 eV for pure TiO_2 anatase (shown in inset).[11,18] It confirms the formation of MoS_2 nanosheets and $MoS_2@TiO_2$ in few-layers range.

3.5 Photocatalytic activity

The photocatalytic behaviour of the prepared samples is investigated by degrading MB under natural sunlight condition. The degradation process is

tested for five different conditions i) self-degradation of MB, i.e., in the absence of any photocatalyst, ii) using MoS_2 nanosheets as photocatalyst in dark and, iii) in presence of sunlight, iv) using $MoS_2@TiO_2$ composite nanosheets as photocatalyst in dark and v) in presence of sunlight. Figures 4(a-e) depicts the UV-Vis spectra (zoomed portion around 665 nm shown in inset) of the

different samples after photocatalytic degradation of MB at an interval of 30 minutes. The characteristic absorption peak of MB occurs near 665 nm and the peak intensity is found to decrease with irradiation time due to the photocatalytic dye degradation owing to the samples.[2] After 180 minutes of irradiation, it is observed that there is very small reduction in
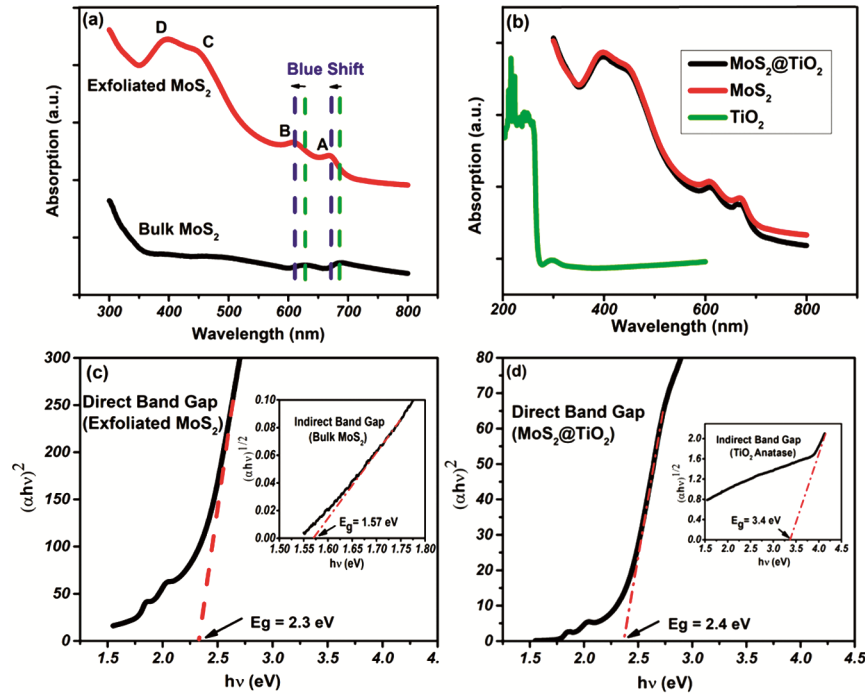
Fig. 3 — UV-Vis spectra of (a) Bulk MoS_2 and MoS_2 nanosheets, (b) pure TiO_2 anatase, $MoS_2@TiO_2$ nanosheets and MoS_2 nanosheets. Tauc plots of (c) Bulk MoS_2 and MoS_2 nanosheets, (d) pure TiO_2 anatase, $MoS_2@TiO_2$ nanosheets.
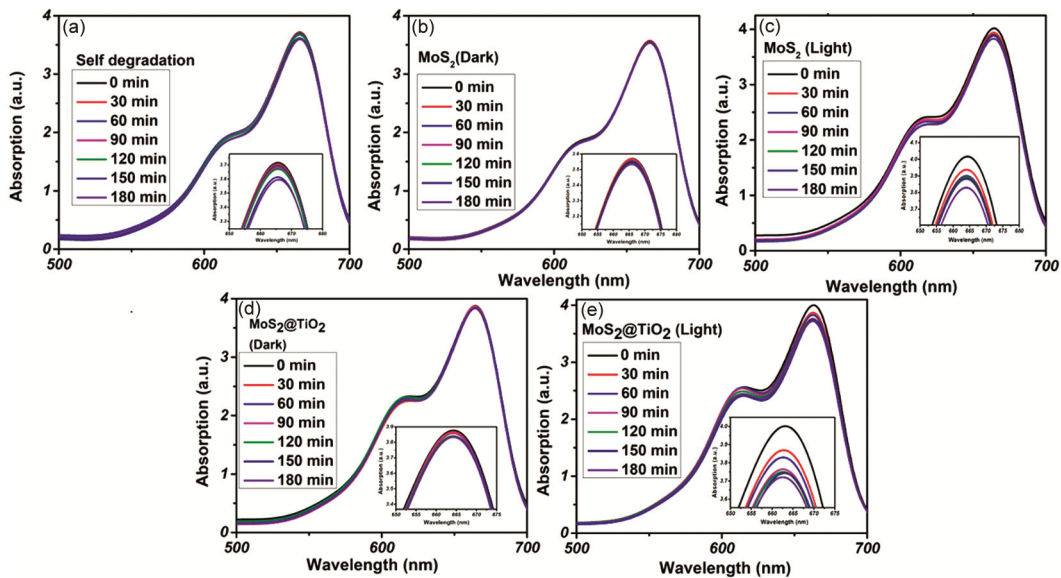
Fig. 4 — UV-Vis spectra of (a) self-degradation of MB, (b) MoS_2 catalyst in dark, (c) MoS_2 catalyst in light, (d) $MoS_2@TiO_2$ catalyst in dark and (e) $MoS_2@TiO_2$ catalyst in light for 180 minutes at an interval of 30 minutes. The region around 665 nm peak in zoomed version is shown in the inset.

absorption peak in the absence of photocatalyst indicating very small self-degradation of MB. By the way of comparison, peak intensity reduction is minimum for dark conditions and maximum in the presence of sunlight especially for the composite sample. Although the surface area of MoS_2 is large, the photogenerated charges recombine faster while it is less in case of anatase TiO_2, thus the composite is showing enhanced photocatalytic activity. Moreover, semiconductors having large band gap are proven to be better photocatalysts than materials having a low bandgap.[10]

Further, the percentage of dye degradation for all the samples is calculated by using the equation

$$D(\%) = \frac{C_0 - C_t}{C_0} \times 100 \qquad \ldots (1)$$

Where, C_0 is the initial dye concentration at time 0 s and C_t is the dye concentration at time t s.

The percentage of photodegradation for all the prepared samples is shown in Fig. 5(a,b). The obtained degradation percentage for the samples are 7.18% (MoS_2@TiO_2 in light) > 4.69 % (MoS_2 in light) > 3.27 % (self-degradation of MB in light) >

1.10 % (MoS_2@TiO_2 in dark) > 1.04 % (MoS_2 in dark). This gives an estimate for the efficiency and potential of samples for photodegradation phenomenon resulting maximum for the composite material MoS_2@TiO_2 in the presence of sunlight irradiation in comparison to pristine MoS_2 nanosheets. Briefly, in dark conditions, the degradation is due to the adsorption of dye on the surface of photocatalysts while in case of illumination, the degradation is due to the multiple reactions between photo-generated electron-hole pairs and organic pollutants in the aqueous medium.[9]

3.6 Photocatalytic degradation mechanism

The mechanism of photocatalysis by the prepared catalysts in degradation process is explained schematically in Fig.6. Under visible light irradiation, electron-hole pairs generation occurs in both MoS_2 and TiO_2 on absorption of photons of optimum energy. In case of pristine MoS_2 nanosheets, the photogenerated electrons (e^-) and holes (h^+) recombine readily in comparison to MoS_2@TiO_2 composite nanosheets. The MoS_2 is placed in such way that its conduction band is at higher energy value
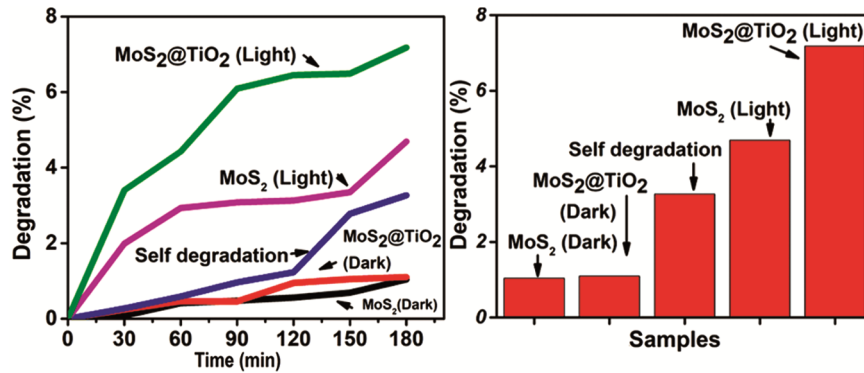
Fig. 5 — Degradation percentage (a) with time and (b) with catalyst samples.
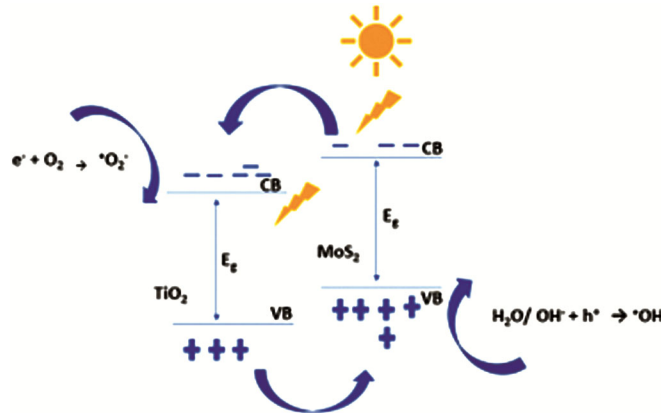
Fig. 6 — Schematic diagram for mechanism of photocatalysis.

than TiO_2. Thus, the electrons transfer from MoS_2 conduction band to TiO_2 conduction band and holes from TiO_2 valence band transfer to MoS_2 valence band. This slows down the recombination process and hence effective utilization of electron-hole pairs. Upon reaction of the holes with water molecules (H_2O) or hydroxyl ions (OH-) hydroxyl radicals (·OH) are produced, while the reaction of electrons with oxygen (O_2) produces superoxide radicals ($·O_2^-$). Thereafter, these radicals undergo chemical reactions with the organic pollutants, i.e., MB decomposing it into non-harmful compounds CO_2 and H_2O.[10]

$$H_2O/OH^- + h^+ \rightarrow ·OH$$
$$e^- + O_2 \rightarrow ·O_2^-$$
$$·OH + MB \rightarrow CO_2 + H_2O$$
$$·O_2^- + MB \rightarrow CO_2 + H_2O$$
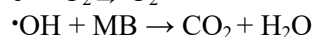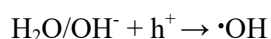
4 Conclusions

Ultrathin, few-layered 2D MoS_2 nanosheets and $MoS_2@TiO_2$ composite nanosheets are exfoliated via grinding-assisted sonication method. It is an easy, efficient and cost-effective technique that can be employed for the scalable synthesis of optimum quality nanosheets. These nanosheets are examined for the photocatalytic activities by decomposing MB under natural sunlight irradiation. The composite ($MoS_2@TiO_2$) nanosheets show enhanced degradation efficiency of 7.18 % in comparison to pristine MoS_2 nanosheets (4.69 %) showing the better potential of composite catalyst. This study incorporates TiO_2 reinforced MoS_2 composite nanosheets, a novel composite catalyst. The composite nanosheets exhibit better photocatalytic results owing to less recombination of photo-generated electron-hole pairs due to transfer of electrons from MoS_2 to TiO_2 and holes from TiO_2 to MoS_2 which is not possible in pristine MoS_2 nanosheets. Moreover, MoS_2 and TiO_2 act as photo harvester in visible and UV range respectively utilizing solar spectrum widely and TiO_2 as co-catalyst for improved charge separation. In conclusion, in case of $MoS_2@TiO_2$, superior absorption of photons, efficient generation, improved separation and transfer of photo-generated electron-hole pairs infer the enhanced photocatalytic performance. This study is helpful in providing $MoS_2@TiO_2$ nanosheets as futuristic candidate for tackling dye pollutants for application in wastewater treatment plants.

References

1   Dharamalingam K, Kumar B A, RamalingamG, Florence S S, Raju K, Kumar P S, Govindaraju S & Thangavel E, *Chemosphere,* 294 (2022) 133725.
2   Sabarinathan M, Harish S, Archana J, Navaneethan M, Ikeda H & Hayakawa Y, *RSC Adv*, 7 (2017) 24754.
3   Saha N, Sarkar A, Ghosh A B,Dutta A K, Bhadu G R, Paul P & Adhikary B, *RSC Adv*, 5(2015) 88848.
4   Das S, Tama A M, Dutta S, Ali M S & Basith M A, *Mater Res Express*, 6 (2019)125079.
5   O'Neill A, Khan U, & Coleman J N, *Chem Mater,* 24 (2012) 2414.
6   Yao Y,Tolentino L, Yang Z, Song X, Zhang W, Chen Y& Wong C, *Adv Funct Mater,* 23 (2013) 3577.
7   Sun J, Li X, Guo W, Zhao M, Fan X, Dong Y, Xu C, Deng J & Fu Y, *Crystals*, 7 (2017) 198.
8   Fujishima A & Honda, *Nature,* 238 (1972).
9   Zhou F,Liu W, Miao Z, & Wang Q, *Chemistry Select*, 4(2019) 7260 –7269.
10 Khan R, Riaz A, Javed S, Rahim J,Akram M A & Mujahid M, *Key Eng Mater*,778 (2018) 137.
11 Mutyala S, Sadiq M M J, Gurulakshmi M, Suresh C, Bhat D K, Shanthi K & Mathiyarasu J, *J Nanosci Nanotechnol*, 20 (2020) 1118.
12 Wang C, Frogley M D, Cinque G, Liu L Q & Barber A H, *Nanoscale*, 00 (2014) 1.
13 Verma R, Gangwar J & Srivastava A K, *RSC Adv*, 7 (2017) 44199.
14 Prabukumar C, Sadiq M M J, Bhat D K& Bhat K U, *AIP Conf Proc*, 1943 (2018) 020084.
15 Lee S K,Chu D, Song D Y, Pak S W & Kim E K, *Nanotechnology*, 28 (2017) 195703.
16 Sarma S &Ray S C, *Appl Surf Sci*,474(2018) 227.
17 Karmakar S, Biswas S &Kumbhakar P, *Opt Mater*, 73(2017) 585.
18 Ramos JrR A, Boratto M H, Li M S, Andrade Scalvi L V, *Mat Res*, 20 (2017) 866.